

How stationary are planetary waves in the Southern Hemisphere?

Elio Campitelli ¹Carolina Vera ^{1,2}Leandro Daz ^{1,2}

¹Centro de Investigaciones del Mar y la Atmosfera, UMI-IFAECI (CONICET-UBA-CNRS)

²Departamento de Ciencias de la Atmsfera y los Ocanos (FCEyN, UBA)

Key Points:

- We devised a quantitative measure of planetary wave stationarity
- In the southern hemisphere planetary waves 2 and 3 have decadal variations in stationarity

Corresponding author: Elio Campitelli, elio.campitelli@cima.fcen.uba.ar

Abstract

Most studies of quasi stationary planetary waves have assumed the quasi stationary nature of southern hemisphere planetary waves based on van Loon and Jenne (1972), which was based on only 2 years of data before the advent of modern reanalysis. In this study, we devised a quantitative measure of planetary wave stationarity and applied it to both hemispheres using the NCEP Reanalysis. We show that in the southern hemisphere planetary wave 1 is highly stationary while planetary waves 2 and 3 have a comparable mixture of stationary and moving components with significant decadal variability. These variations can be used to study variability in surface forcing responses caused either by the strength of the forcing or the sensitivity of the atmosphere to the forcing.

1 Introduction

Zonal asymmetries of extratropical circulation in the Southern Hemisphere (hereafter called as “planetary waves”) strongly modulate weather systems and regional climate through latitudinal transport of heat, humidity, and momentum (REFS), and by contributing to the development of blocking events (e.g. Trenberth & Mo, 1985).

In Rossby wave theory, stationary waves are those with zero frequency or phase velocity (Holton & Hakim, 2012). In practice, however, most studies have assumed the quasi-stationary nature of southern hemisphere planetary waves based on van Loon and Jenne (1972). In this foundational study, the authors analyzed data only from two years, from 1957 and 1958 and found that while extratropical waves with wavenumber 1 to 6 had comparable amplitudes in daily fields, only wavenumbers 1 and 3 contributed significantly to the climatological field. From that, they concluded that only waves 1 and 3 recur consistently in the same location and thus have a significant quasi-stationary component on top of a “moving” component. This was a qualitative conclusion and to our knowledge no study has quantified the level of stationarity of each wavenumber.

After more than four decades from the publication of van Loon and Jenne (1972), and considering the current availability of different global reanalysis datasets, in this study we assess the stationarity features of planetary waves in the southern hemisphere, and extend van Loon and Jenne (1972)’s methodology into a quantitative measure of planetary wave stationarity, which we apply to both hemispheres.

2 Methods

2.1 Planetary waves

We define *planetary waves* as waves that extend along a full latitude circle. *Zonal waves* (ZW) are planetary waves of the “instantaneous” fields and *quasi-stationary waves* (QS), planetary waves of the time-mean field such that:

$$\text{ZWk}(t) = A_{\text{ZWk}}(t) \cos [k\lambda - \alpha_{\text{ZWk}}(t)] \quad (1)$$

$$\overline{\text{ZWk}(t)} = \text{QSk} = A_{\text{QSk}} \cos (k\lambda - \alpha_{\text{QSk}}) \quad (2)$$

where k is wavenumber, λ longitude, and A_x and α_x , amplitude and phase, respectively. $\text{ZWk}(t)$ depends on time, but not QSk .

These definitions depend on which are the “instantaneous fields” and the averaging time-scales. A dataset of 365 daily mean fields defines 365 daily zonal waves and one annual quasi-stationary wave but 12 monthly quasi-stationary waves (per level and latitude). A 30 year dataset of monthly mean fields define 360 monthly zonal waves and one 30-year quasi-stationary wave. Monthly planetary waves are quasi-stationary waves in the first case and zonal waves in the second, remarking that the definition of quasi-stationary waves is dependent of the time sampling considered.

2.2 Stationarity

From the properties of the superposition of waves we can deduce that, in general, the stationary phase α_{QSk} does not equal $\overline{\alpha_{\text{ZWk}}}$ and the stationary amplitude A_{QSk} is less or equal to $\overline{A_{\text{ZWk}}}$ (Pain, 2005).

We use this latter property and use the quotient between A_{QS} and $\overline{A_{\text{ZW}}}$ as a measure of quasi-stationary wave stationarity such as:

$$\hat{S} = \frac{A_{\text{QS}}}{\overline{A_{\text{ZW}}}} \quad (3)$$

For a sample of n completely random waves, the expected value of \hat{S} is $n^{-1/2}$ because the average amplitude of the sum of n waves with random phases and mean am-

plitude A is $An^{-1/2}$ (Pain, 2005). For completely stationary waves, \hat{S} is equal to 1 regardless of sample size.

\hat{S} is used –sometimes as $2/\pi \arcsin(\hat{S})$ (Singer, 1967)– in the meteorological literature in the context of wind steadiness (e.g Hiscox, Miller, & Nappo, 2010). To our knowledge this is the first time to be applied to the study of atmospheric waves.

\hat{S} could be equivalent formulated as

$$\hat{S} = \frac{\sum_t A_{ZW}(t) \cos[\alpha_{ZW}(t) - \alpha_{qs}]}{\sum_t A_{ZW}(t)} \quad (4)$$

The numerator represents the sum of the zonal waves amplitudes projected onto the direction of the quasi-stationary wave. Waves that deviate from that direction decrease the overall stationarity in proportion to their amplitude. This definition of stationarity depends on the phase distribution and its relationship with amplitude. And because it does not depend on the propagating properties of waves, it’s a statistical – rather than dynamical– property.

We used Equation 4 to compute a timeseries of quasi-stationary wave stationarity. We first calculated α_{qs} for each month and then applied Equation 4 with a 15-year rolling window approximated using loess regression with degree 0.

2.3 Data

We use monthly geopotential fields from the NCEP/NCAR Reanalysis (Kalnay et al., 1996) for the period 1948 to 2017 and compute one quasi-stationary wave for the whole period for each month, level and wavenumber. Amplitude and phase for each wavenumber was estimated by fitting a fourier transform for each latitude circle, level and monthly record. We also analyzed data from ERA Interim (Uppala et al., 2011) and confirmed that we get similar results.

We analyzed the data using the statistical programming language R (R Core Team, 2018), using data.table (Dowle & Srinivasan, 2018) and metR (Campitelli, 2018) packages to read and transform it and ggplot2 package (Wickham, 2016) to make the plots. The source code is available as Figshare repository (Campitelli, 2019).

3 Results

Figure 1 shows the seasonal cycle of the amplitude of planetary waves at 50°S and 50°N using monthly fields from the NCEP/NCAR reanalysis (Kalnay et al., 1996) between 1948 and 2017. We computed the left column (A_{QS}) as the amplitude of the average geopotential field for each month, level and wavenumber, and the right column ($\overline{A_{ZW}}$) as the average amplitude of the 70 individual fields.

Figure 1a shows that at 50°N for the three wavenumbers A_{QS} and $\overline{A_{ZW}}$ have a similar seasonal cycle with similar vertical extent. In the southern hemisphere, however, this is true only for wavenumber 1 (Figure 1b). A_{QS2} has much lower values than $\overline{A_{ZW2}}$ and its seasonal cycle is less defined. A_{QS3} has a smaller magnitude than $\overline{A_{ZW3}}$ and even though their overall structure is similar (one relative maximum in February-March in the middle troposphere and another in July-August that extends to the lower stratosphere), they differ in the details. A_{QS3} has a local minimum in November that is absent in $\overline{A_{ZW3}}$. The relative contribution of each wavenumber is also different. While $\overline{A_{ZW2}}$ dominates over $\overline{A_{ZW3}}$ in the stratosphere and is of similar magnitude in the troposphere, A_{QS3} dominates over A_{QS2} throughout the year and in every level except in the aforementioned November minimum.

The differences between A_{QS} and $\overline{A_{ZW}}$ are quantified in Figure 2, which shows \hat{S} for wavenumbers 1 to 3 computed using Equation 3 at 50°N and 50°S.

At 50°N planetary waves 1, 2 and 3 are highly stationary in almost every month and level, and even more so planetary wave 1 at 50°S.

In the southern hemisphere, planetary wave 2 stationarity has a semiannual cycle. It reaches its maximum in April and in August-September, decreasing to a deep minimum centered in June. Planetary wave 3 stationarity peaks in February and slowly decreases towards a November deep minimum after which increases sharply.

As we computed \hat{S} using the whole period for Figure 2, it represents the mean stationarity between 1948 and 2017. To analyse changes of stationarity over time, we computed \hat{S} using 10 year overlapping intervals for each wavenumber at both studied latitudes (Figure 3). Planetary wave stationarity remained high and constant for wavenumbers 1 to 3 at 50°N and 1 at 50°S but wavenumbers 2 and 3 at 50°S show interdecadal variations.

Planetary wave 2 stationarity oscillated around 0.5 with maximums in the 50's, 70's and 00's. Planetary wave 3 stationarity jumped from zero to more than 0.5 in less than five years in the 50's and then oscillated around 0.6 with a strong maximum in the late 80's.

Results from ERA Interim (not shown) coincide during the period of overlap (1979-2018), suggesting that the observed decadal variations are not an artifact of the reanalysis. For the later period, the sudden shift in planetary wave 3 stationarity between 1950 and 1960 is probably spurious and we couldn't find it using data from ERA 20C (not shown).

4 Conclusions

We used a quantitative measure of planetary wave stationarity to show that in the southern hemisphere planetary wave 1 stationarity is high and constant throughout the year and period, while waves 2 and 3 vary both in intraseasonal and interdecadal timescales. In the northern hemisphere, planetary wave stationarity is higher and varies much less.

Planetary waves can be both forced by the surface and excited by internal variability. Assuming that the later process will not result in a phase preference, higher stationarity would be evidence of stronger forcing or, more strictly, stronger forcing response. In the northern hemisphere, topography and thermal contrasts are the main forcings of planetary waves (REF), which explains their highly and not variable stationary nature. In the southern hemisphere, only planetary wave 1 seems to be the result of mainly surface forcings. Planetary waves 2 and 3 seem to be composed of a comparable mix of internal variability and surface forcing components.

Interannual and intradecadal variability in planetary wave stationarity may serve to study variability in surface forcing responses caused either by the strength of the forcing or the sensitivity of mean state of the atmosphere.

Since in the southern hemisphere the amplitude of the mean planetary wave can differ greatly from the mean amplitude of planetary waves, care must be taken when interpreting the literature. Some studies analyze the former (e.g. van Loon & Jenne, 1972, Quintanar and Mechoso (1995), Raphael (2004)) while others analyze the later (e.g. Rao, Fernandez, & Franchito, 2004, Turner, Hosking, Bracegirdle, Phillips, and Marshall (2017), Irving and Simmonds (2015)). For instance, Irving and Simmonds (2015) compare their

planetary wave activity index with Raphael (2004)’s wave 3 index and conclude that the later cannot account for events with waves far removed from their climatological position. However, being an index of the zonal wave component in phase with the quasi-stationary wave, this is by design.

The explorations of both zonal waves and quasi-stationary waves can lead to novel levels of analysis. For example, Smith and Kushner (2012) used their phase relationship to show that linear interference between the zonal waves 1 and quasi-stationary wave 1 was related to vertical wave activity transport at the tropopause. Here, we showed it can be used to define a metric of stationarity of quasi-stationary waves, but other applications are also possible.

References

- Campitelli, E. (2018). `metr`: Tools for easier analysis of meteorological fields [Computer software manual]. Retrieved from <https://github.com/eliocamp/metr> (R package version 0.2.9000)
- Campitelli, E. (2019). *How stationary are planetary waves in the Southern Hemisphere?: supplementary data*. Retrieved from <http://dx.doi.org/10.6084/m9.figshare.7599890> doi: 10.6084/m9.figshare.7599890
- Dowle, M., & Srinivasan, A. (2018). `data.table`: Extension of ‘data.frame’ [Computer software manual]. Retrieved from <http://r-datatable.com> (R package version 1.11.9)
- Hiscox, A. L., Miller, D. R., & Nappo, C. J. (2010). Plume meander and dispersion in a stable boundary layer. *Journal of Geophysical Research: Atmospheres*, 115(D21). Retrieved from <https://agupubs.onlinelibrary.wiley.com/doi/abs/10.1029/2010JD014102> doi: 10.1029/2010JD014102
- Holton, J. R., & Hakim, G. J. (2012). *An introduction to dynamic meteorology: Fifth edition*. doi: 10.1016/C2009-0-63394-8
- Irving, D., & Simmonds, I. (2015, dec). A novel approach to diagnosing Southern Hemisphere planetary wave activity and its influence on regional climate variability. *Journal of Climate*, 28(23), 9041–9057. Retrieved from <http://journals.ametsoc.org/doi/10.1175/JCLI-D-15-0287.1> doi: 10.1175/JCLI-D-15-0287.1
- Kalnay, E., Kanamitsu, M., Kistler, R., Collins, W., Deaven, D., Gandin, L.,

- 186 ... Joseph, D. (1996). The NCEP/NCAR 40-year reanalysis project.
 187 *Bulletin of the American Meteorological Society*, 77(3), 437–471. doi:
 188 10.1175/1520-0477(1996)077<0437:TNYRP>2.0.CO;2
- 189 Pain, H. (2005). Simple Harmonic Motion. In *The physics of vibrations and waves*
 190 (p. 570). doi: 10.1002/0470016957
- 191 Quintanar, A. I., & Mechoso, C. R. (1995). Quasi-stationary waves in the Southern
 192 Hemisphere. Part I: observational data. *Journal of Climate*, 8(11), 2659–2672.
 193 doi: 10.1175/1520-0442(1995)008<2659:QSWITS>2.0.CO;2
- 194 R Core Team. (2018). R: A language and environment for statistical computing
 195 [Computer software manual]. Vienna, Austria. Retrieved from [https://www.R-](https://www.R-project.org/)
 196 [project.org/](https://www.R-project.org/)
- 197 Rao, V. B., Fernandez, J. P. R., & Franchito, S. H. (2004). Quasi-stationary waves
 198 in the southern hemisphere during El Nina and La Nina events. *Annales Geo-*
 199 *physicae*, 22(3), 789–806.
- 200 Raphael, M. N. (2004, dec). A zonal wave 3 index for the Southern Hemisphere.
 201 *Geophysical Research Letters*, 31(23), 1–4. Retrieved from [http://doi.wiley](http://doi.wiley.com/10.1029/2004GL020365)
 202 [.com/10.1029/2004GL020365](http://doi.wiley.com/10.1029/2004GL020365) doi: 10.1029/2004GL020365
- 203 Singer, I. A. (1967, dec). Steadiness of the Wind. *Journal of Applied Meteorology*,
 204 6(6), 1033–1038. Retrieved from [http://journals.ametsoc.org/doi/abs/](http://journals.ametsoc.org/doi/abs/10.1175/1520-0450(1967)006<1033:SOTW>2.0.CO;2)
 205 [10.1175/1520-0450\(1967\)006<1033:SOTW>2.0.CO;2](http://journals.ametsoc.org/doi/abs/10.1175/1520-0450(1967)006<1033:SOTW>2.0.CO;2)
 206 [.CO;2](http://journals.ametsoc.org/doi/abs/10.1175/1520-0450(1967)006<1033:SOTW>2.0.CO;2) doi: 10.1175/1520-0450(1967)006<1033:SOTW>2.0.CO;2
- 207 Smith, K. L., & Kushner, P. J. (2012). Linear interference and the initiation of ex-
 208 tratropical stratosphere-troposphere interactions. *Journal of Geophysical Re-*
 209 *search Atmospheres*, 117(13), 1–16. doi: 10.1029/2012JD017587,2012
- 210 Trenberth, K. E., & Mo, K. C. (1985). Blocking in the Southern Hemi-
 211 sphere. *Monthly Weather Review*, 113(1), 3–21. Retrieved from [http://](http://journals.ametsoc.org/doi/abs/10.1175/1520-0493(1985)113<0003:BITSH>2.0.CO;2)
 212 [journals.ametsoc.org/doi/abs/10.1175/1520-0493\(1985\)113<0003:BITSH>2.0.CO;2](http://journals.ametsoc.org/doi/abs/10.1175/1520-0493(1985)113<0003:BITSH>2.0.CO;2)
 213 [}29113\(1985\)113<0003:BITSH>2.0.CO;2](http://journals.ametsoc.org/doi/abs/10.1175/1520-0493(1985)113<0003:BITSH>2.0.CO;2) doi: 10.1175/
 214 [1520-0493\(1985\)113<0003:BITSH>2.0.CO;2](http://journals.ametsoc.org/doi/abs/10.1175/1520-0493(1985)113<0003:BITSH>2.0.CO;2)
- 215 Turner, J., Hosking, J. S., Bracegirdle, T. J., Phillips, T., & Marshall, G. J. (2017).
 216 Variability and trends in the Southern Hemisphere high latitude, quasi-
 217 stationary planetary waves. *International Journal of Climatology*, 37(5),
 218 2325–2336. doi: 10.1002/joc.4848

- 219 Uppala, S. M., Healy, S. B., Balmaseda, M. A., de Rosnay, P., Isaksen, L., van de
220 Berg, L., . . . Morcrette, J.-J. (2011). The ERA-Interim reanalysis: configura-
221 tion and performance of the data assimilation system. *Quarterly Journal of the*
222 *Royal Meteorological Society*, 137(656), 553–597. doi: 10.1002/qj.828
- 223 van Loon, H., & Jenne, R. L. (1972). The Zonal Harmonic Standing Waves in the
224 Southern Hemisphe. *Journal of Geophysical Research*, 77(6), 992–1003.
- 225 Wickham, H. (2016). *ggplot2: Elegant graphics for data analysis*. Springer-Verlag
226 New York. Retrieved from <http://ggplot2.org>

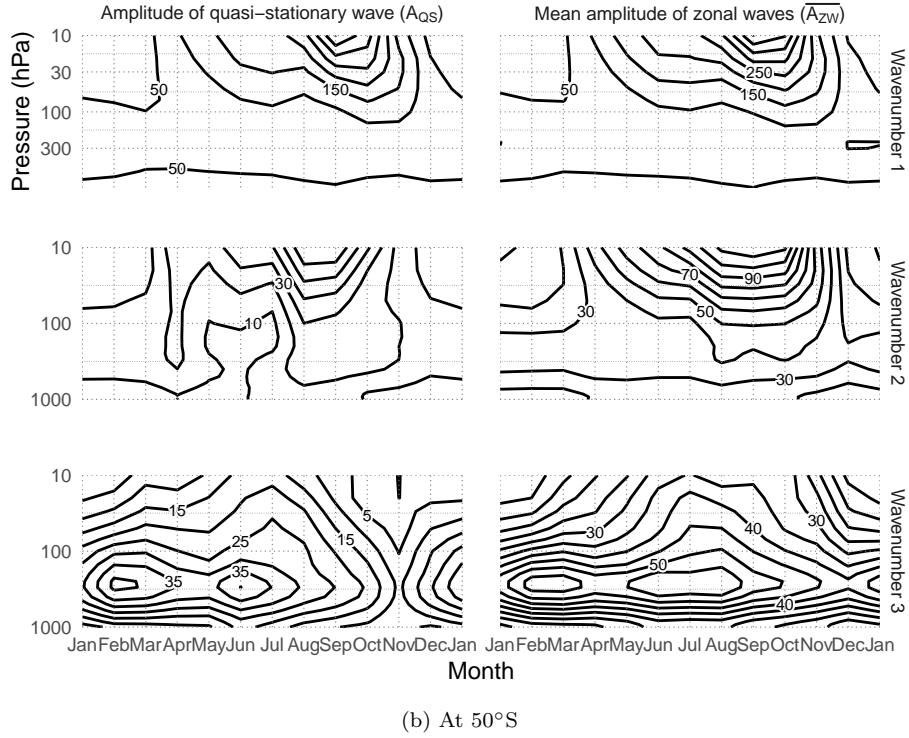
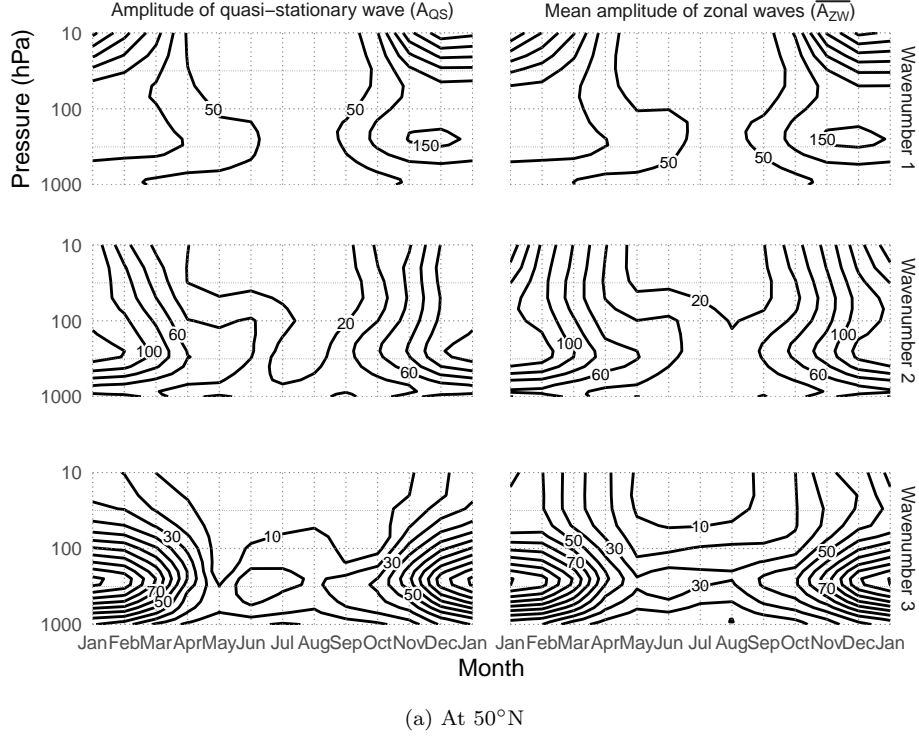


Figure 1: Seasonal cycle of amplitude of the geopotential planetary waves 1, 2 and 3 (top, middle and bottom rows, respectively) computed as the mean amplitude of the monthly waves ($\overline{A_{ZW}}$, left column) the amplitude of the mean wave (A_{QSk} , right column)

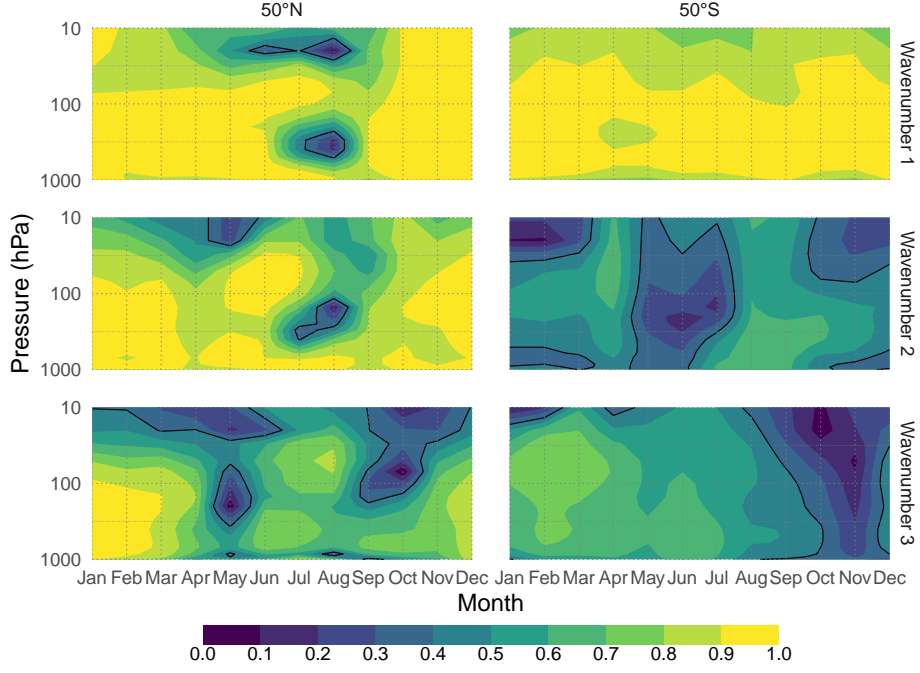


Figure 2: Seasonal cycle of stationarity of the geopotential planetary waves 1, 2 and 3 (top, middle and bottom rows, respectively) at 50°N and 50°S (left and right columns, respectively) computed using Equation 3. The black line marks $\hat{S} = 0.4$ for reference.

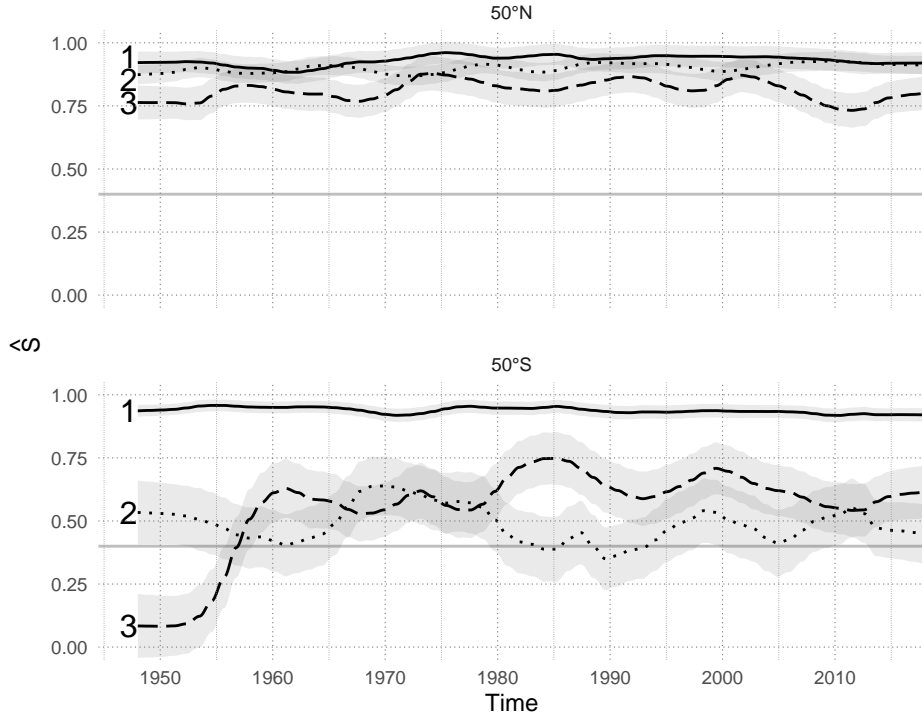


Figure 3: Stationarity for wavenumbers 1 to 3 at 50°N and 50°S (top and bottom panels, respectively) at 500hPa.